Northern Hemisphere monsoon response to mid-Holocene orbital forcing and greenhouse gas-induced global warming

Article

Accepted Version

Northern Hemisphere monsoon response to mid-Holocene orbital forcing and greenhouse gas-induced global warming

Roberta D'Agostino[1]

Jürgen Bader[1,2]

Simona Bordoni[3]

David Ferreira[4]

Johann Jungclaus[1]

[1]Max Planck Institute for Meteorology, Hamburg, Germany.

[2]Uni Climate, Uni Research and the Bjerknes Centre for Climate Research, Bergen, Norway.

[3]California Institute of Technology, Pasadena, California.

[4]Department of Meteorology, University of Reading, United Kingdom

Key Points:

- Different mechanisms mediate the response of Northern Hemisphere monsoons under future global warming and mid-Holocene forcing.
- Northern Hemisphere monsoons intensify more strongly in mid-Holocene than in future climate despite a larger warming in the latter.
- As an emergent constraint for future projections, tropical circulation weakening limits monsoon rainfall increase with global warming.

Corresponding author: Roberta D'Agostino, Max Planck Institute for Meteorology, Bundesstr. 53, 20146, Hamburg, Germany, `roberta.dagostino@mpimet.mpg.de`

Abstract

Precipitation and circulation patterns of Northern Hemisphere monsoons are investigated in Coupled Model Intercomparison Project phase 5 simulations for mid-Holocene and future climate scenario rcp8.5. Although both climates exhibit Northern Hemisphere warming and enhanced inter-hemispheric thermal contrast in boreal summer, changes in the spatial extent and rainfall intensity in future climate are smaller than in mid-Holocene for all Northern Hemisphere monsoons except the Indian monsoon. A decomposition of the moisture budget in thermodynamic and dynamic contributions suggests that under future global warming the weaker response of the African, Indian and North American monsoons results from a compensation between both components. The dynamic component, primarily constrained by changes in net energy input over land, determines instead most of the mid-Holocene land monsoonal rainfall response.

1 Introduction

The mid-Holocene was a period around 6,000 years ago, when insolation changes driven by Earth's axis precession changes resulted in a general warming of the Northern Hemisphere (NH), an enhanced insolation seasonality and a stronger inter-hemispheric thermal contrast compared with present-day boreal summer (Zhao & Harrison, 2012). In agreement with expectations based on recent theories of monsoons (Schneider et al., 2014), these insolation-driven temperature changes resulted in a robust increase in monsoonal rainfall during the last interglacial and the mid-Holocene in North Africa (Weldeab et al., 2007; Tjallingii et al., 2008), India (Schulz et al., 1998; Fleitmann et al., 2003), East Asia (Liu & Ding, 1998; Yuan et al., 2004; Wang et al., 2008; Lézine et al., 2011; Hély & Lézine, 2014; Tierney & Pausata, 2017) and northernmost South America (Haug et al., 2001) as shown by proxy reconstructions. This wettening tendency is also observed in a number of climate simulations from the Paleoclimate Model Intercomparison Project (PMIP) (Zhao et al., 2005; Zhao & Harrison, 2012) under mid-Holocene forcing, despite difficulties in reproducing the magnitude and northward expansion of rainfall as suggested by proxy data, particularly over the Sahara (Braconnot et al., 1999; Liu et al., 2007; Braconnot et al., 2012; Harrison et al., 2015; Boos & Korty, 2016). Some recent studies show better agreement with proxies on mid-Holocene precipitation in models that account for interactive vegetation or realistic vegetation cover over the Sahara (Vamborg et al., 2010; Swann et al., 2014; Pausata et al., 2016; Egerer et al., 2018; Lu et al., 2018), but sim-

ulations with precipitation and vegetation changes consistent with proxies have yet to be achieved.

Similar to mid-Holocene, the Representative Concentration Pathway global warming scenario rcp8.5 projects a warming of the Northern relative to the Southern Hemisphere and an enhanced inter-hemispheric thermal contrast resulting from stronger warming over land than over ocean (Sutton et al., 2007; Compo & Sardeshmukh, 2009; Jones et al., 2013; Acosta Navarro et al., 2017). These elements all support a tendency toward increased global monsoon rainfall strength and extent (Trenberth et al., 2000; Hsu et al., 2012, 2013; Kitoh et al., 2013; Lee & Wang, 2014) associated with reinforced low-level moisture convergence (Hsu et al., 2012; Kitoh et al., 2013; Lee & Wang, 2014). On a regional scale, evaluation of Coupled Model Intercomparison Project phase 3 and 5 (CMIP3 and CMIP5) simulations has indicated a wettening of the Asian monsoon (Kitoh et al., 2013; Endo & Kitoh, 2014) but has shown poor agreement in the African monsoon region because of competing effects of CO_2 increase and SST biases on the modelled West African monsoon response (Biasutti, 2013; Gaetani et al., 2017). Projections of the North American monsoon remain more inconclusive, with most models projecting a delay in the monsoon season with no robust changes in its summer mean intensity (Cook & Seager, 2013; Seth et al., 2013, 2011). The extent to which this might be a result of existing biases in the simulations of the present-day monsoon climatology remains a topic of debate (Pascale et al., 2017).

Despite a different global mean temperature response, the mean warming and the enhanced inter-hemispheric temperature contrast would suggest a strengthening and widening of NH monsoons in both climates relative to pre-industrial conditions (Tab. S2). Nevertheless, how similar the resulting regional monsoon responses are, remains unknown.

The energetic view of monsoons as moist energetically direct circulations tightly connected to the global Hadley cell (Bordoni & Schneider, 2008; Schneider et al., 2014; Biasutti et al., 2018) rather than as sea-breeze circulations driven by land-ocean temperature contrast (Webster & Fasullo, 2002; Fasullo & Webster, 2003; Fasullo, 2012; Gadgil, 2018) might provide some insight into the differing response of NH monsoons to mid-Holocene and rcp8.5 scenario. In this view, monsoons are fundamental components of the tropical overturning circulation, and, like the global mean Hadley cell, they export moist static energy (MSE) away from their ascending branches and precipitation max-

ima. If eddy energy fluxes are negligible, this implies that net energy input (NEI) into the atmospheric column given by the difference between top-of-atmosphere radiative and surface energy fluxes is primarily balanced by divergence of vertically integrated mean MSE flux (Chou et al., 2001; Merlis et al., 2013; Boos & Korty, 2016, see Eq. (3) below). Not surprisingly, the MSE budget has therefore provided the theoretical framework to understand the response of monsoons to different surface heat capacity (i.e. ocean versus land) (Chou et al., 2001), changes in atmospheric dynamics (Tanaka et al., 2005; Vecchi & Soden, 2007), in tropical tropospheric stability (Neelin et al., 2003), and in vegetation (Kutzbach et al., 1996; Claussen & Gayler, 1997; Broström et al., 1998; Claussen et al., 2013).

Changes in inter-hemispheric contrast in NEI, such as for instance those driven by precession-induced insolation changes, require anomalous meridional energy transport to restore energy balance. To the extent that during the summer most of this transport is accomplished by monsoonal circulations (Heaviside & Czaja, 2013; Walker, 2017), this would imply a shift of the monsoonal circulation ascending branches and precipitation maxima into the hemisphere with increased NEI and, possibly, an associated circulation strengthening (Schneider et al., 2014; Bischoff et al., 2017). It is important to note, however, that the MSE budget constrains the energy transport rather than the circulation strength itself (Merlis et al., 2013; Hill et al., 2015). The degree to which changes in energy transport implied by a given radiative forcing are accomplished through just changes in circulation strength or also changes in energy stratification (or gross moist stability, Neelin and Held, 1987) is not fully understood.

Here, we investigate the NH monsoon response in CMIP5 simulations under rcp8.5 and mid-Holocene forcing factors. Given the stronger thermal contrast between hemispheres and land versus ocean in rcp8.5 than in mid-Holocene one might expect that monsoon rainfall and extent would be greater in the former than in the latter. However, we will show that the opposite is true. Mechanisms of this differing monsoon response are investigated by decomposing the anomalous moisture budget in thermodynamic and dynamic components. The dynamic component is further related to NEI changes, to better understand why monsoons respond differently to different climate forcings and to explore to what extent the mid-Holocene may be considered as an analogue of future greenhouse gas-induced warming.

2 Data and Methods

We leverage mid-Holocene, piControl and rcp8.5 experiments that are available in CMIP5 archives. We use the first ensemble member (r1i1p1) of nine available models with all three experiments (i.e., bcc-csm-1-1, CCSM4, CNRM-CM5, CSIRO-Mk3-6-0, FGOALS-g2, HadGEM2-ES, IPSL-CM5A-LR, MIROC-ESM and MRI-CGCM3, see Table SI1). All datasets are interpolated to a common $1° \times 1.25°$ latitude/longitude grid and to 17 pressure levels.

June to September (JJAS) climatologies are calculated for the last 30 years of rcp8.5, for the period 1850 - 2005 of piControl and for the last 100 years of mid-Holocene simulations. September is also included in the summer season, to account for seasonality delays in the Hadley and monsoonal circulations in both mid-Holocene and rcp8.5 (Seth et al., 2010; Dwyer et al., 2012; Seth et al., 2013; D'Agostino et al., 2017).

Changes in monsoon extent and strength are assessed using the following metrics: the monsoon extent is the land-only area where annual precipitation range, defined as the difference between summer and winter rainfall, exceeds 2 mm/day for each monsoon domain. The selected threshold warrants a concentrated summer rainy season and distinguishes monsoons from year-round rainy regimes (Zhou et al., 2008; Liu et al., 2009; Hsu et al., 2012). Choosing different definitions to calculate land-monsoon area (e.g. local summer precipitation exceeding 35%, 40%, 50% of the annual rainfall) does not significantly affect our results. The monsoon strength is the average summer rainfall calculated in each monsoon domain, specifically (see boxes in Fig. 1):

1. African monsoon (5° to 23.3° N, 20° W to 40° E).
2. Indian monsoon (5° to 23.3° N, 70° to 120° E).
3. North American monsoon (5° to 30° N, 120° W to 40° W).

We also consider the whole NH tropical land-monsoon area (NHM, 5° to 30° N, 0 to 360° E). We exclude from our analyses the East Asian monsoon because its dynamics is related to shifts of the Pacific Subtropical High and interactions between the jet-stream and the Asian topography rather than to ITCZ seasonal migration and regional Hadley cell dynamics (Chen & Bordoni, 2014; Zhisheng et al., 2015). Following Trenberth and Guillemot (1995), the linearized anomalous moisture budget is decomposed into thermodynamic, dynamic components and a residual (*Res*) as:

$$\rho_w g \delta(P - E) \ = \ - \int_0^{p_s} \nabla \cdot (\delta \overline{q} \ \overline{\mathbf{u}}_{\mathrm{piControl}}) \ dp \ - \int_0^{p_s} \nabla \cdot (\overline{q}_{\mathrm{piControl}} \delta \overline{\mathbf{u}}) \ dp \ - Res, \quad (1)$$

where overbars indicate monthly means, $(P - E)$ is precipitation minus evaporation, p is pressure, q is specific humidity, $\overline{\mathbf{u}}$ is the horizontal vector wind, and ρ_w is the water density. δ indicates the difference between each experiment (mid-Holocene or rcp8.5) and the reference climate (piControl) as:

$$\delta(\cdot) \ = \ (\cdot)_{\mathrm{mid-Holocene \ or \ rcp8.5}} \ - \ (\cdot)_{\mathrm{piControl}}. \quad (2)$$

In Eq. (1), the first term on the right-hand side is the thermodynamic contribution (TH): it represents changes in moisture flux convergence arising from changes in moisture, which generally follow the Clausius-Clapeyron relation for negligible relative humidity changes (e.g. Held and Soden, 2006). The second term in Eq. (1), the dynamic contribution (DY), involves changes in winds with unchanged moisture, and is mostly related to changes in the mean atmospheric flow. The third term describes the residual (Res) which accounts for transient eddy contribution and surface quantities as described in the Supplementary Information.

Changes in the DY contribution to monsoonal precipitation changes are related to patterns of anomalous NEI, as any anomalous NEI in monsoonal regions will require changes in MSE export by the mean circulation in steady state:

$$\nabla \cdot \{\overline{\mathbf{u}h}\} = NEI = R_{TOA} - F_{sfc}, \quad (3)$$

where $\{\overline{\mathbf{u}h}\}$ is the vertically integrated MSE flux, R_{TOA} the net top-of-atmosphere radiative fluxes and F_{sfc} the sum of the surface radiative and turbulent enthalpy fluxes.

3 Results

The future rcp8.5 and the past mid-Holocene climates are associated, respectively, with a strong (+4.2 K) and a weak (+0.3 K) global warming signal relative to piControl (Fig. 1, upper panels; Table S2). They also exhibit higher inter-hemispheric thermal contrasts (+10.0 K and +9.7 K compared to +9.2 K for piControl, see Table S2). However, the precipitation difference between rcp8.5 and mid-Holocene (Fig. 1, lower panel)

reveals a complex pattern of relative drying and wettening, reflective of a general tendency towards land drying and ocean wettening in rcp8.5, and land wettening and ocean drying in mid-Holocene.

To explain these differences in the precipitation response, we analyze the anomalous moisture budget of the two climates relative to piControl. This analysis shows how changes in net precipitation $\delta(P-E)$ (see Eq. (1)) are primarily due to changes in precipitation alone, with changes in evaporation being negligible both in the multi-model mean (Figure S1 and S2) and in each individual model (not shown). Relative to piControl, precipitation in the African and Indian monsoons generally increases in mid-Holocene, while it decreases in the North American monsoon and increases in the Indian monsoon in rcp8.5. Figure 2 shows a general wettening of African and Indian monsoons in mid-Holocene relative to piControl, while in rcp8.5 the North American monsoon dries and the Indian monsoon wettens. The drying in the North American monsoon seen under rcp8.5 in the models considered in this study is at odds with previously published studies, which suggest no robust changes in the mean monsoon precipitation, but is in agreement with simulations in which SST biases in the North Atlantic are corrected with flux adjustment (Pascale et al., 2017). These ensemble mean $(P-E)$ changes are robust as they occur in at least 8 out 9 models considered here (stippled areas in Fig. 2), but models disagree on the magnitude of these changes. However, while in mid-Holocene models robustly produce wettening in the African equatorial rain belt and the sub-Saharan region, particularly in those models with active land module (i.e. bcc-csm1-1, CCSM4, CNRM-CM5, IPSL-CM5A-LR, FGOALS-g2, Had-GEM-ES, MIROC-ESM), there is less consensus on net precipitation changes in rcp8.5. Only CCSM4 shows a wettening of equatorial Africa; other models show decreased or no change in monsoonal precipitation (not shown).

It is noteworthy that, on a global scale (including changes over land as well as over oceans), rcp8.5 exhibits a robust shift of tropical precipitation towards the near-equatorial ocean relative to piControl (Fig. 2c). This tendency is also consistent with the projected squeezing of rain belts around the equator and the narrowing of the ITCZ in rcp8.5 (Byrne & Schneider, 2016). These findings however highlight that global ITCZ changes are not a good indicator of the land monsoon changes.

It is readily apparent from Figs. 1 and 2 that the mid-Holocene monsoon response is not a weaker version of the rcp8.5 response. Even more surprisingly, the simulated land monsoon changes are almost systematically smaller in rcp8.5 than in mid-Holocene, despite stronger global mean temperature increase and a slightly larger inter-hemispheric thermal contrast in the former than in the latter. In fact, both extent and strength of individual monsoons and the global NH land monsoon are projected to increase more in mid-Holocene than in rcp8.5. The notable exception to this general pattern is the Indian monsoon, whose strength increases more in rcp8.5 (Tab. 1).

To explain why the monsoon response is weaker under future global warming relative to the mid-Holocene, we decompose $\delta(P-E)$ in TH and DY contributions as described in Section 2. Each of these components is shown in Figure S3 and S4; Results are summarized in Fig. 3 by averaging these components in each monsoon domain, where annual-range precipitation exceed 2 mm/day. The magnitude of the residual relative to the other components is also shown.

Fig. 3 reveals a striking contrast in the response in the two climates: in mid-Holocene, the DY term dominates the anomalous moisture budget in the African and Indian monsoon regions and in the overall NH monsoon domain. Only in the North American monsoon region does this term contribute marginally to the anomalous moisture budget (Fig. 3, and Fig. S3b). The DY component increases NH land precipitation through increased moisture convergence there (Fig. S3; see methods in Supplementary Information). Likewise, drying over near-equatorial oceans is associated with weaker wind convergence, especially in the Atlantic sector. Therefore, the enhanced African and Indian monsoonal rainfall in mid-Holocene is due to a strengthening of the mean flow. On the other hand, the TH component plays a secondary role in the mid-Holocene net precipitation increase in all monsoon domains, except in the North American monsoon (Fig. 3a and Fig. S3 a and c). On average, the TH and DY terms tend to reinforce each other, both contributing to a wettening tendency.

In contrast, the overall weaker wettening in future rcp8.5 projections results from a compensation between the DY term and the TH term (where the latter moistens monsoons as the climate warms) (Fig. 3b and Fig. S4). The substantial drying of the North American monsoon arises mainly from a strong weakening of the mean circulation (DY term, Table 1). On the other hand, the TH and the DY components feature strong spa-

tial variations in the Indian monsoon region: the TH plays a major role in the wetting tendency over the eastern Indian peninsula, and is responsible for the strong drying on its western part (Fig. S4). However, averaging over the entire domain, the TH term dominates over the DY term, and drives an overall wettening.

These analyses suggest therefore that the wettening and northward shift of NH monsoons in mid-Holocene arises mainly from the strengthening of the mean circulation. On the other hand, the weak monsoon response to anthropogenic forcing in rcp8.5 relative to mid-Holocene is mainly due to a compensation between the thermodynamically driven wettening and a dynamically driven drying, as already pointed out by some previous studies (Seager et al., 2010, 2014; Endo & Kitoh, 2014).

Tropical circulation weakening with warming (i.e. weakening of the DY component in all considered monsoons) is a consequence of increased stability in the tropics where temperature lapse rates follow moist adiabats (Held & Soden, 2006). Over tropical and subtropical continents, the stability increase is not compensated by increases in low-level MSE which reduces convection and moisture convergence from oceans, with an associated reduction in land monsoonal rainfall (Fasullo, 2012). The projected monsoonal circulation weakening relative to mid-Holocene hence represents a constraint for monsoonal rainfall: precipitation squeezes around the tropical ocean in rcp8.5 as the static stability increases, the circulation weakens and continental moisture convergence decreases. Unlike what is seen in rcp8.5, the strengthening of the circulation in mid-Holocene allows for increased moisture convergence over land monsoon regions, with a shift of the tropical precipitation from ocean to land and stronger monsoonal rainfall than projected in rcp8.5.

To further understand, at least qualitatively, the different response of land-ocean monsoonal rainfall in the two climates, we analyze changes in NEI in mid-Holocene and rcp8.5 relative to piControl (Fig. 3 and 4). In mid-Holocene, the NEI response is mainly positive over NH continents relative to piControl primarily because of precession-induced insolation changes (Fig. 4a). On the other hand, patterns of anomalous NEI are of opposite sign in rcp8.5, with positive values over the tropical ocean. Hence, to compensate for these NEI changes, the mid-Holocene atmospheric circulation needs to export more energy away from land regions, through a strengthening of the associated DY term (Fig. 3). In rcp8.5, increased stability and the absence of such energetic forcing over NH lands,

²⁶⁵ where the energy budget is controlled by the top of the atmosphere radiation due to the

²⁶⁶ small thermal inertia of land (Neelin & Held, 1987), cause a weakening of the monsoonal

²⁶⁷ circulation an overall decrease of tropical land rainfall relative to mid-Holocene. Fig. 3

²⁶⁸ shows in fact a systematic NEI increase of ~ 8 W/m² in mid-Holocene, compared to a

²⁶⁹ weak change (< 1 W/m²) in rcp8.5.

4 Discussion and Conclusions

²⁷¹ Here, we have investigated mechanisms of monsoon moistening and expansion in

²⁷² two climates, mid-Holocene and future climate scenario rcp8.5. In both climates, the sim-

²⁷³ ulated NH summer monsoon rainfall is stronger and monsoon area wider than in the pre-

²⁷⁴ industrial era. However, the projected monsoon response to global warming is weaker

²⁷⁵ than in the simulated past, despite a much larger global warming in the former than in

²⁷⁶ the latter.

²⁷⁷ In rcp8.5, the NH land monsoon is expected to become wetter relative to pre-industrial

²⁷⁸ conditions because the atmospheric specific humidity increase leads to enhanced precip-

²⁷⁹ itation (thermodynamic effect). Additionally, the Hadley circulation is projected to ex-

²⁸⁰ pand and weaken in the future (Frierson et al., 2007; Lu et al., 2007; Seidel et al., 2008;

²⁸¹ D'Agostino et al., 2017) following the widening and the slowdown already observed in

²⁸² recent decades (Hu & Fu, 2007; Birner, 2010; Davis & Rosenlof, 2012; Nguyen et al., 2013;

²⁸³ D'Agostino & Lionello, 2017). This weakens the dynamic term of the moisture budget.

²⁸⁴ Therefore, the weak monsoonal rainfall response with global warming generally results

²⁸⁵ from a compensation between the thermodynamic and dynamic terms. The degree of

²⁸⁶ compensation differs strongly among monsoon regions. For instance, in the Indian mon-

²⁸⁷ soon the TH component overwhelms the DY component, giving rise to an overall wet-

²⁸⁸ tening; in the North American monsoon, the DY component is dominant and respon-

²⁸⁹ sible for a significant drying.

²⁹⁰ Unlike what happens under greenhouse gas-induced warming, the strengthening

²⁹¹ of the mean atmospheric flow is the dominant mechanism behind the wettening and widen-

²⁹² ing of NH monsoons in mid-Holocene. The circulation brings more rainfall over land than

²⁹³ over ocean, expanding the total NH land-monsoon area further northward than in rcp8.5.

²⁹⁴ In fact, the dynamic response reinforces the thermodynamically driven wettening in mid-

²⁹⁵ Holocene; in contrast the two components partially cancel each other in rcp8.5.

Advances in our theoretical understanding of monsoons allows us to link dynamically-induced precipitation changes to changes in NEI (Chou et al., 2001; Neelin et al., 2003; Byrne & Schneider, 2016). In this framework, monsoonal circulations, as part of the global tropical overturning, export MSE away from their ascending branches. In steady state, the net MSE flux divergence balances the NEI. Therefore to the extent that energy stratification does not change significantly, changes in NEI need to be compensated for by changes in circulation strength. Hence, the different monsoon responses in the two climates can ultimately be related to changes in the forcing itself, which influences differently the NEI over land and over ocean. In fact, the shortwave forcing, which dominates the mid-Holocene, exhibits a stronger land-ocean contrast than the longwave perturbation associated with greenhouse gas increases in rcp8.5 (Fig. S5). In mid-Holocene, the stronger cross-equatorial atmospheric circulation and the enhanced dynamic term are a result of increased energetic input over the continents: the atmospheric circulation must be stronger in order to export energy away from these regions in the past climate. The absence of such energetic forcing over NH lands in rcp8.5 relative to mid-Holocene results in a relative weakening of mean circulation and hence of the associated precipitation. The strengthening of the dynamic component, therefore, represents a key ingredient for monsoon widening and wettening in mid-Holocene. The weakening of the tropical circulation with global warming limits the projected expansion and intensification of the monsoon systems. The degree of compensation between the thermodynamic and dynamic responses with warming remains highly uncertain and might contribute significantly to the inter-model spread in CMIP5 simulations (Stocker et al., 2014).

This process-oriented study takes an important step towards improving our understanding of monsoon dynamics, quantifying the important role of atmospheric circulation changes in monsoonal precipitation changes by comparing and contrasting past and future climates. Our results highlight that mean surface warming and inter-hemispheric contrast in surface warming are poor indicators of the monsoonal precipitation response. Rather, the monsoon response is constrained by the integrated energy balance, which accounts for changes at the surface as well as at the top of the atmosphere. This explains why the mid-Holocene does not represent an analogue for future warming.
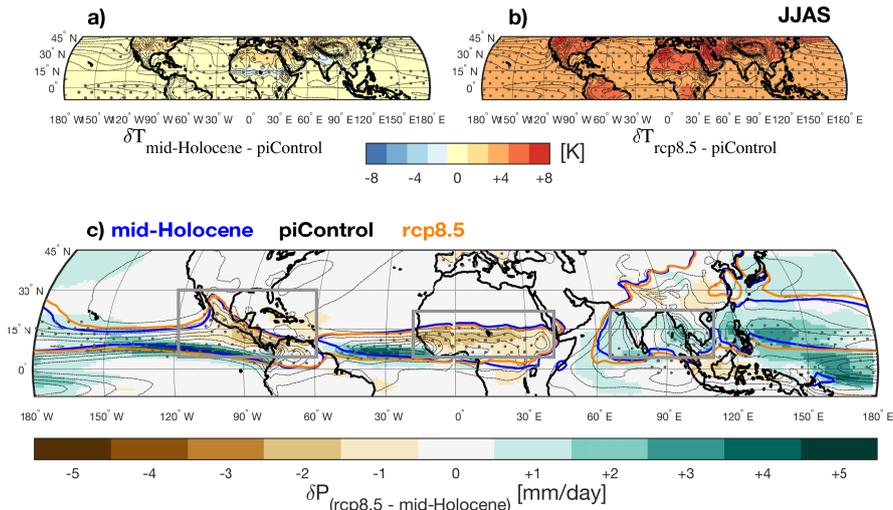
Figure 1. Surface temperature difference between mid-Holocene (a) and rcp8.5 (b) and piControl in June-to-September (JJAS) ensemble means (shading). Precipitation difference between rcp8.5 and mid-Holocene JJAS ensemble means (c, shading). Black dashed lines in every panel show the piControl as reference (contour interval 2 K for temperature and 2 mm/day for precipitation). Orange and blue bold lines in c) show areas within which the annual precipitation range (JJAS minus DJFM) exceeds 2 mm/day for rcp8.5 and mid-Holocene, respectively. Grey boxes indicate the North American, African and Indian monsoon domains. Stippling indicates areas where at least 8 out of 9 models agree on the sign of the change.

Acknowledgments

Figure 2. Net precipitation difference between the mid-Holocene (a) and the rcp8.5 (c) relative to *piControl* in June-to-September (JJAS) ensemble means (shading). PiControl is also shown as reference (b). Black dashed lines in each panel show the piControl as reference (contour interval 20 W/m^2). Stippling indicates areas where at least where 8 out of 9 models agree on the sign of the change.

References

Acosta Navarro, J. C., Ekman, A. M., Pausata, F. S., Lewinschal, A., Varma, V.,
    Seland, Ø., ... Riipinen, I. (2017). Future response of temperature and precipitation to reduced aerosol emissions as compared with increased greenhouse gas
    concentrations. *Journal of Climate*, *30*(3), 939–954.

Biasutti, M. (2013). Forced Sahel rainfall trends in the CMIP5 archive. *Journal of
    Geophysical Research: Atmospheres*, *118*(4), 1613–1623.

Biasutti, M., Voigt, A., Boos, W. R., Braconnot, P., Hargreaves, J. C., Harrison,
    S. P., ... Schumacher, C. (2018). Global energetics and local physics as drivers
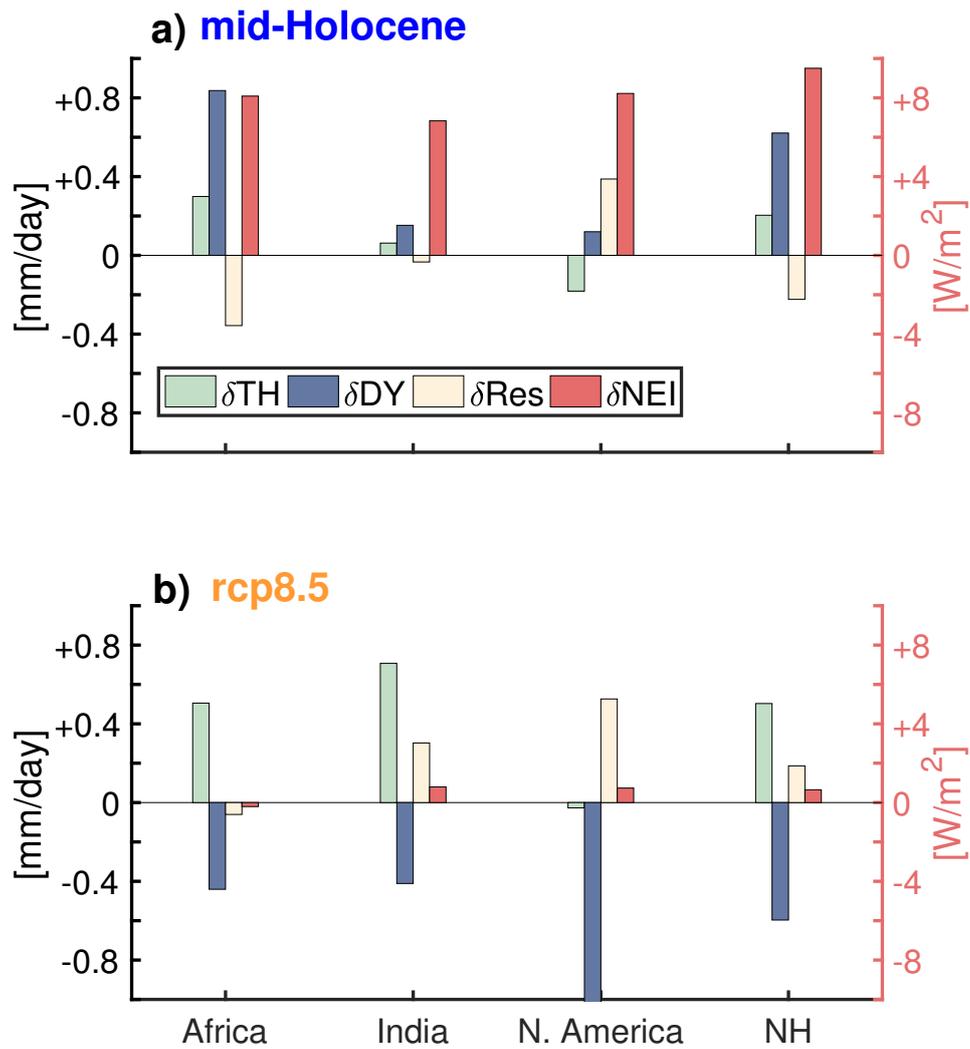
Figure 3. Regionally averaged Net Energy Input (NEI - red axis) changes and changes in thermodynamic (δ TH) and dynamic (δDY) components of the moisture budget, as well as its residual (δRes) (see Eq.1) for mid-Holocene (a) and rcp8.5 (b) (black axis). Note that 8 out of 9 models agree on the sign of the change.

of past, present and future monsoons. *Nature Geoscience*, *11*(6), 392.

Birner, T.   (2010).   Recent widening of the tropical belt from global tropopause statistics: Sensitivities.   *J. Geophys. Res.*, *115*, D23109.   doi: 10.1029/ 2010JD014664

Bischoff, T., Schneider, T., & Meckler, A. N.   (2017).   A conceptual model for the response of tropical rainfall to orbital variations.   *Journal of Climate*, *30*(20), 8375–8391.
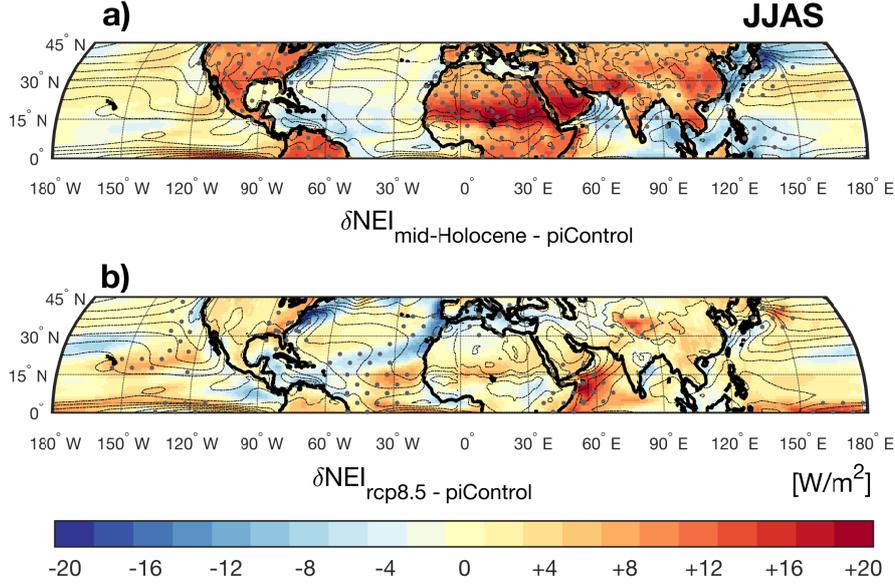
Figure 4. Net energy input (NEI) difference between mid-Holocene (a) and rcp8.5 (b) relative to piControl in June-to-September (JJAS) ensemble means (shading). Stippling indicates areas where at least 8 out of 9 models agree on the sign of the change.

Table 1. Changes in mid-Holocene and rcp8.5 land monsoon extent and strength relative to piControl. Standard errors for piControl models are reported in brackets. The monsoon extent is calculated inside each monsoon domain where the difference between JJAS and DJFM precipitation exceeds 2 mm/day, as shown in solid lines in Fig. 1.

Monsoons	Extent (10^6 Km)			Strength (mm/day)			ITCZ (lat. degs)			$\phi_{Pr>2mm/day}$		
	piControl	*mid-Holocene*	*rcp8.5*	*piControl*	*mid-Holocene*	*rcp8.5*	*piControl*	*mid-Holocene*	*rcp8.5*	*piControl*	*mid-Holocene*	*rcp8.5*
African	5.2 ($\pm$0.7)	+15.4%	+4.4%	5.3 ($\pm$11.0)	+20.3%	+1.2%	7.5	8.4	7.5	14.2	15.4	14.2
Indian	3.1 ($\pm$0.4)	+9.2%	+7.4%	8.5 ($\pm$1.3)	+1.6%	+4.8%	11.5	11.6	11.4	21.8	22.9	22.6
North American	2.8 ($\pm$0.5)	+3.7%	-4.3%	5.8 ($\pm$1.3)	+7.8%	-5.8%	8.1	8.3	7.7	20.1	20.0	21.6
NH	9.3 ($\pm$1.0)	+15.1%	+4.8%	7.0 ($\pm$0.5)	+1.1%	-1.8%	7.9	7.9	7.2	19.2	19.6	18.2

Boos, W. R., & Korty, R. L. (2016). Regional energy budget control of the intertropical convergence zone and application to mid-Holocene rainfall. *Nature Geoscience*, *9*(12), 892.

Bordoni, S., & Schneider, T. (2008). Monsoons as eddy-mediated regime transitions of the tropical overturning circulation. *Nature Geoscience*, *1*(8), 515.

Braconnot, P., Harrison, S. P., Kageyama, M., Bartlein, P. J., Masson-Delmotte, V., Abe-Ouchi, A., ... Zhao, Y. (2012). Evaluation of climate models using palaeoclimatic data. *Nature Climate Change*, *2*(6), 417–424.

Braconnot, P., Joussaume, S., Marti, O., & De Noblet, N. (1999). Synergistic feedbacks from ocean and vegetation on the African monsoon response to mid-Holocene insolation. *Geophysical Research Letters*, *26*(16), 2481–2484.

Broström, A., Coe, M., Harrison, S., Gallimore, R., Kutzbach, J., Foley, J., . . . Behling, P. (1998). Land surface feedbacks and palaeomonsoons in Northern Africa. *Geophysical Research Letters*, *25*(19), 3615–3618.

Byrne, M. P., & Schneider, T. (2016). Narrowing of the ITCZ in a warming climate: Physical mechanisms. *Geophysical Research Letters*, *43*(21).

Chen, J., & Bordoni, S. (2014). Orographic effects of the Tibetan Plateau on the East Asian summer monsoon: An energetic perspective. *Journal of Climate*, *27*(8), 3052–3072.

Chou, C., Neelin, J., & Su, H. (2001). Ocean-atmosphere-land feedbacks in an idealized monsoon. *Quarterly Journal of the Royal Meteorological Society*, *127*(576), 1869–1891.

Claussen, M., Bathiany, S., Brovkin, V., & Kleinen, T. (2013). Simulated climate–vegetation interaction in semi-arid regions affected by plant diversity. *Nature Geoscience*, *6*(11), 954.

Claussen, M., & Gayler, V. (1997). The greening of the Sahara during the mid-Holocene: results of an interactive atmosphere-biome model. *Global Ecology and Biogeography Letters*, 369–377.

Compo, G. P., & Sardeshmukh, P. D. (2009). Oceanic influences on recent continental warming. *Climate Dynamics*, *32*(2-3), 333–342.

Cook, B., & Seager, R. (2013). The response of the North American Monsoon to increased greenhouse gas forcing. *Journal of Geophysical Research: Atmospheres*, *118*(4), 1690–1699.

D'Agostino, R., Lionello, P., Adam, O., & Schneider, T. (2017). Factors controlling Hadley circulation changes from the Last Glacial Maximum to the end of the 21st century. *Geophysical Research Letters*, *44*(16), 8585–8591.

Davis, S. M., & Rosenlof, K. H. (2012). A multidiagnostic intercomparison of tropical-width time series using reanalyses and satellite observations. *Journal of Climate*, *25*(4), 1061–1078.

Dwyer, J. G., Biasutti, M., & Sobel, A. H. (2012). Projected changes in the seasonal cycle of surface temperature. *Journal of Climate*, *25*(18), 6359–6374.

D'Agostino, R., & Lionello, P. (2017). Evidence of global warming impact on the evolution of the Hadley Circulation in ECMWF centennial reanalyses. *Climate Dynamics*, *48*(9-10), 3047–3060.

Egerer, S., Claussen, M., & Reick, C. H. (2018). Rapid increase in simulated North Atlantic dust deposition due to fast change of Northwest African landscape during Holocene. *Climate of the Past*, *14*, 1051–1066.

Endo, H., & Kitoh, A. (2014). Thermodynamic and dynamic effects on regional monsoon rainfall changes in a warmer climate. *Geophysical Research Letters*, *41*(5), 1704–1711.

Fasullo, J. (2012). A mechanism for land–ocean contrasts in global monsoon trends in a warming climate. *Climate dynamics*, *39*(5), 1137–1147.

Fasullo, J., & Webster, P. (2003). A hydrological definition of Indian monsoon onset and withdrawal. *Journal of Climate*, *16*(19), 3200–3211.

Fleitmann, D., Burns, S. J., Mudelsee, M., Neff, U., Kramers, J., Mangini, A., & Matter, A. (2003). Holocene forcing of the Indian monsoon recorded in a stalagmite from southern Oman. *Science*, *300*(5626), 1737–1739.

Frierson, D. M., Lu, J., & Chen, G. (2007). Width of the Hadley cell in simple and comprehensive general circulation models. *Geophysical Research Letters*, *34*(18).

Gadgil, S. (2018). The monsoon system: Land–sea breeze or the ITCZ? *Journal of Earth System Science*, *127*(1), 5.

Gaetani, M., Flamant, C., Bastin, S., Janicot, S., Lavaysse, C., Hourdin, F., . . . Bony, S. (2017). West African monsoon dynamics and precipitation: The competition between global SST warming and CO2 increase in CMIP5 idealized simulations. *Climate Dynamics*, *48*(3-4), 1353–1373.

Harrison, S. P., Bartlein, P., Izumi, K., Li, G., Annan, J., Hargreaves, J., . . . Kageyama, M. (2015). Evaluation of CMIP5 palaeo-simulations to improve climate projections. *Nature Climate Change*, *5*(8), 735.

Haug, G. H., Hughen, K. A., Sigman, D. M., Peterson, L. C., & Röhl, U. (2001). Southward migration of the intertropical convergence zone through the Holocene. *Science*, *293*(5533), 1304–1308.

Heaviside, C., & Czaja, A. (2013). Deconstructing the Hadley cell heat transport. *Quarterly Journal of the Royal Meteorological Society*, *139*(677), 2181–2189.

Held, I. M., & Soden, B. J. (2006). Robust responses of the hydrological cycle to global warming. *Journal of Climate*, *19*(21), 5686–5699.

Hély, C., & Lézine, A.-M. (2014). Holocene changes in African vegetation: Tradeoff between climate and water availability. *Climate of the Past*, *10*(2), 681–686.

Hill, S. A., Ming, Y., & Held, I. M. (2015). Mechanisms of forced tropical meridional energy flux change. *Journal of Climate*, *28*(5), 1725–1742.

Hsu, P.-c., Li, T., Luo, J.-J., Murakami, H., Kitoh, A., & Zhao, M. (2012). Increase of global monsoon area and precipitation under global warming: A robust signal? *Geophysical Research Letters*, *39*(6).

Hsu, P.-c., Li, T., Murakami, H., & Kitoh, A. (2013). Future change of the global monsoon revealed from 19 CMIP5 models. *Journal of Geophysical Research: Atmospheres*, *118*(3), 1247–1260.

Hu, Y., & Fu, Q. (2007). Observed poleward expansion of the Hadley circulation since 1979. *Atmospheric Chemistry and Physics*, *7*(19), 5229–5236.

Jones, G. S., Stott, P. A., & Christidis, N. (2013). Attribution of observed historical near–surface temperature variations to anthropogenic and natural causes using CMIP5 simulations. *Journal of Geophysical Research: Atmospheres*, *118*(10), 4001–4024.

Kitoh, A., Endo, H., Krishna Kumar, K., Cavalcanti, I. F., Goswami, P., & Zhou, T. (2013). Monsoons in a changing world: A regional perspective in a global context. *Journal of Geophysical Research: Atmospheres*, *118*(8), 3053–3065.

Kutzbach, J., Bonan, G., Foley, J., & Harrison, S. (1996). Vegetation and soil feedbacks on the response of the African monsoon to orbital forcing in the early to middle Holocene. *Nature*, *384*(6610), 623.

Lee, J.-Y., & Wang, B. (2014). Future change of global monsoon in the CMIP5. *Climate Dynamics*, *42*(1-2), 101–119.

Lézine, A.-M., Hély, C., Grenier, C., Braconnot, P., & Krinner, G. (2011). Sahara and Sahel vulnerability to climate changes, lessons from Holocene hydrological data. *Quaternary Science Reviews*, *30*(21-22), 3001–3012.

Liu, J., Wang, B., Ding, Q., Kuang, X., Soon, W., & Zorita, E. (2009). Centennial variations of the global monsoon precipitation in the last millennium: Results from ECHO-G model. *Journal of Climate*, *22*(9), 2356–2371.

Liu, Z., & Ding, Z. (1998). Chinese loess and the paleomonsoon. *Annual review of*

earth and planetary sciences, *26*(1), 111–145.

Liu, Z., Wang, Y., Gallimore, R., Gasse, F., Johnson, T., Adkins, J., . . . Jacob, R. (2007). Simulating the transient evolution and abrupt change of Northern Africa atmosphere–ocean–terrestrial ecosystem in the Holocene. *Quaternary Science Reviews*, *26*(13-14), 1818–1837.

Lu, J., Vecchi, G., & Reichler, T. (2007). Expansion of the hadley cell under global warming. *Geophysical Research Letters*, *34*(6).

Lu, Z., Miller, P., Zhang, Q., Li, Q., Wårlind, D., Nieradzik, L., . . . Smith, B. (2018). Dynamic vegetation simulations of the mid-Holocene Green Sahara. *Geophysical Research Letters*.

Merlis, T., Schneider, T., Bordoni, S., & Eisenman, I. (2013). Hadley circulation response to orbital precession. Part I: Aquaplanets. *Journal of Climate*, *26*(3), 740–753.

Neelin, J., Chou, C., & Su, H. (2003). Tropical drought regions in global warming and El-niño teleconnections. *Geophysical Research Letters*, *30*(24).

Neelin, J., & Held, I. (1987). Modeling tropical convergence based on the moist static energy budget. *Monthly Weather Review*, *115*(1), 3–12.

Nguyen, H., Evans, A., Lucas, C., Smith, I., & Timbal, B. (2013). The Hadley Circulation in reanalyses: Climatology, variability, and change. *Journal of Climate*, *26*(10).

Pascale, S., Boos, W. R., Bordoni, S., Delworth, T., Kapnick, S., Murakami, H., . . . Zhang, W. (2017). Weakening of the North American monsoon with global warming. *Nature Climate Change*, *7*(11), 806.

Pausata, F., Messori, G., & Zhang, Q. (2016). Impacts of dust reduction on the northward expansion of the African monsoon during the Green Sahara period. *Earth and Planetary Science Letters*, *434*, 298–307.

Schneider, T., Bischoff, T., & Haug, G. H. (2014). Migrations and dynamics of the intertropical convergence zone. *Nature*, *513*(7516), 45–53.

Schulz, H., von Rad, U., & Erlenkeuser, H. (1998). Correlation between Arabian Sea and Greenland climate oscillations of the past 110,000 years. *Nature*, *393*(6680), 54.

Seager, R., Liu, H., Henderson, N., Simpson, I., Kelley, C., Shaw, T., . . . Ting, M. (2014). Causes of increasing aridification of the Mediterranean region in

response to rising greenhouse gases. *Journal of Climate*, *27*(12), 4655–4676.

Seager, R., Naik, N., & Vecchi, G. A. (2010). Thermodynamic and dynamic mechanisms for large-scale changes in the hydrological cycle in response to global warming. *Journal of Climate*, *23*(17), 4651–4668.

Seidel, D. J., Fu, Q., Randel, W. J., & Reichler, T. J. (2008). Widening of the tropical belt in a changing climate. *Nature geoscience*, *1*(1), 21–24.

Seth, A., Rauscher, S. A., Biasutti, M., Giannini, A., Camargo, S. J., & Rojas, M. (2013). CMIP5 projected changes in the annual cycle of precipitation in monsoon regions. *Journal of Climate*, *26*(19), 7328–7351.

Seth, A., Rauscher, S. A., Rojas, M., Giannini, A., & Camargo, S. J. (2011). Enhanced spring convective barrier for monsoons in a warmer world? *Climatic Change*, *104*(2), 403–414.

Seth, A., Rojas, M., & Rauscher, S. A. (2010). CMIP3 projected changes in the annual cycle of the South American monsoon. *Climatic Change*, *98*(3-4), 331–357.

Stocker, T. F., Qin, D., Plattner, G.-K., Tignor, M., Allen, S. K., Boschung, J., . . . Midgley, P. M. (2014). *Climate change 2013: The physical science basis.* Cambridge University Press Cambridge, UK, and New York.

Sutton, R. T., Dong, B., & Gregory, J. M. (2007). Land/sea warming ratio in response to climate change: IPCC AR4 model results and comparison with observations. *Geophysical Research Letters*, *34*(2).

Swann, A. L., Fung, I. Y., Liu, Y., & Chiang, J. C. (2014). Remote vegetation feedbacks and the mid-Holocene Green Sahara. *Journal of Climate*, *27*(13), 4857–4870.

Tanaka, H., Ishizaki, N., & Nohara, D. (2005). Intercomparison of the intensities and trends of Hadley, Walker and monsoon circulations in the global warming projections. *SOLA*, *1*, 77–80.

Tierney, J. E., & Pausata, F. S. (2017). Rainfall regimes of the Green Sahara. *Science advances*, *3*(1), e1601503.

Tjallingii, R., Claussen, M., Stuut, J.-B. W., Fohlmeister, J., Jahn, A., Bickert, T., . . . Röhl, U. (2008). Coherent high-and low-latitude control of the northwest African hydrological balance. *Nature Geoscience*, *1*(10), 670.

Trenberth, K. E., & Guillemot, C. J. (1995). Evaluation of the global atmospheric

moisture budget as seen from analyses. *Journal of Climate*, *8*(9), 2255–2272.

Trenberth, K. E., Stepaniak, D. P., & Caron, J. M.   (2000).   The global monsoon as seen through the divergent atmospheric circulation.   *Journal of Climate*, *13*(22), 3969–3993.

Vamborg, F., Brovkin, V., & Claussen, M.   (2010).   The effect of a dynamic background albedo scheme on Sahel/Sahara precipitation during the mid-holocene. *Climate of the Past Discussions*, *6*, 2335–2370.

Vecchi, G. A., & Soden, B. J.   (2007).   Global warming and the weakening of the tropical circulation. *Journal of Climate*, *20*(17), 4316–4340.

Walker, J.   (2017).   *Seasonal and interannual variability in South Asian monsoon dynamics* (Unpublished doctoral dissertation).   California Institute of Technology.

Wang, Y., Cheng, H., Edwards, R. L., Kong, X., Shao, X., Chen, S., . . . An, Z. (2008).   Millennial and orbital-scale changes in the East Asian monsoon over the past 224,000 years. *Nature*, *451*(7182), 1090.

Webster, P., & Fasullo, J.   (2002).   Monsoon— dynamical theory.   *Encycl. Atmos. Sci.*, 1370–1385.

Weldeab, S., Lea, D. W., Schneider, R. R., & Andersen, N.   (2007).   155,000 years of west African monsoon and ocean thermal evolution.   *science*, *316*(5829), 1303–1307.

Yuan, D., Cheng, H., Edwards, R. L., Dykoski, C. A., Kelly, M. J., Zhang, M., . . . Wu, J.   (2004).   Timing, duration, and transitions of the last interglacial Asian monsoon. *Science*, *304*(5670), 575–578.

Zhao, Y., Braconnot, P., Marti, O., Harrison, S., Hewitt, C., Kitoh, A., . . . Weber, S.   (2005).   A multi-model analysis of the role of the ocean on the African and Indian monsoon during the mid-Holocene.   *Climate Dynamics*, *25*(7-8), 777–800.

Zhao, Y., & Harrison, S. (2012). Mid-Holocene monsoons: A multi-model analysis of the inter-hemispheric differences in the responses to orbital forcing and ocean feedbacks. *Climate Dynamics*, *39*(6), 1457–1487.

Zhisheng, A., Guoxiong, W., Jianping, L., Youbin, S., Yimin, L., Weijian, Z., . . . Jiangyu, M.   (2015).   Global monsoon dynamics and climate change.   *Annual Review of Earth and Planetary Sciences*, *43*, 29–77.

584   Zhou, T., Zhang, L., & Li, H. (2008). Changes in global land monsoon area and to-

585   tal rainfall accumulation over the last half century.   *Geophysical Research Let-*

586   *ters*, *35*(16).